

## Communications to the Editor

### Cytochrome P-450 Model (Porphinato)(thiolato)iron(III) Complexes with Single and Double NH···S Hydrogen Bonds at the Thiolate Site

Norikazu Ueyama,\* Nami Nishikawa, Yusuke Yamada,  
Taka-aki Okamura, and Akira Nakamura\*

Department of Macromolecular Science  
Graduate School of Science, Osaka University  
Toyonaka, Osaka 560, Japan

Received July 5, 1996

Cytochrome P-450 contains a cysteine thiolate ligand at the axial position of (porphinato)iron(III) core. The axial thiolate has been shown to promote the heterolysis of the coordinated dioxygen upon sequential donation of electron and proton.<sup>1–3</sup> The crystallographic structure of cytochrome P-450<sub>cam</sub> reported by Poulos et al.<sup>4</sup> has suggested the presence of weak double NH···S hydrogen bonds between S of Cys 357 and two amide NHs of Gly 359 and Gln 360, as shown in Figure 1a. Recently, the presence of two clear NH···S hydrogen bonds was reported for the crystal structure of chloroperoxidase.<sup>5</sup> Similar hydrogen bonds are found in the active site of P-450<sub>BM-3</sub>,<sup>6</sup> P-450<sub>terp</sub>,<sup>7</sup> and P-450<sub>eryF</sub>.<sup>8</sup> For P-450<sub>cam</sub>, a molecular dynamics simulation from the reported crystallographic structure results in the shortening of the NH···S hydrogen bond distances.<sup>9</sup> Furthermore, comparison of the Protein Data Bank crystallographical structural parameters at the active sites of substrate-bound P-450<sub>cam</sub> with substrate-free P-450<sub>cam</sub><sup>10</sup> indicates shorter N···S distance at the active site of the substrate-bound P-450<sub>cam</sub> accompanied by a positive shift of the reported redox potential.<sup>11</sup> A remarkable effect on the electrochemical properties by NH···S hydrogen bond have already been revealed by us for various metal thiolate complexes<sup>12–14</sup> as well as iron-sulfur proteins.<sup>15–17</sup> In order

(1) Higuchi, T.; Uzu, S.; Hirobe, M. *J. Am. Chem. Soc.* **1990**, *112*, 7051–7053.

(2) Higuchi, T.; Shimada, K.; Maruyama, N.; Hirobe, M. *J. Am. Chem. Soc.* **1993**, *115*, 7551–7552.

(3) Dawson, J. H. *Science* **1988**, *240*, 435–439.

(4) Poulos, T. L.; Finzel, B. C.; Howard, A. J. *J. Mol. Biol.* **1987**, *195*, 687–700.

(5) Sundaramoorthy, M.; Turner, J.; Poulos, T. L. *Structure* **1995**, *3*, 1367–1377.

(6) Li, H.; Poulos, T. L. *Acta Crystallogr.* **1995**, *D51*, 21–32.

(7) Hasemann, C. A.; Ravichandran, K. G.; Peterson, J. A.; Deisenhofer, J. *J. Mol. Biol.* **1994**, *236*, 1169–1185.

(8) Cupp-Vickery, J. R.; Poulos, T. L. *Nat. Struct. Biol.* **1995**, *2*, 144–153.

(9) A BIOGRAF soft ware (Molecular Simulation Inc.) was used for the molecular mechanics and dynamics calculations that were carried out under  $\epsilon = 7$  and 38 at 300 K.

(10) Poulos, T. L.; Finzel, B. C.; Howard, A. J. *Biochemistry* **1986**, *25*, 5314–5322.

(11) Fisher, M. T.; Sligar, S. G. *J. Am. Chem. Soc.* **1985**, *107*, 5018–5019.

(12) Ueyama, N.; Okamura, T.; Nakamura, A. *J. Chem. Soc., Chem. Commun.* **1992**, 1019–1020.

(13) Ueyama, N.; Okamura, T.; Nakamura, A. *J. Am. Chem. Soc.* **1992**, *114*, 8129–8137.

(14) Ueyama, N.; Terakawa, T.; Nakata, M.; Nakamura, A. *J. Am. Chem. Soc.* **1983**, *105*, 7098.

(15) Watenpugh, K. D.; Sieker, L. C.; Jensen, L. H. *J. Mol. Biol.* **1979**, *131*, 509.

(16) Tsukihara, T.; Fukuyama, K.; Nakamura, M.; Katsube, Y.; Kanaka, N.; Kakudo, M.; Hase, T.; Wada, K.; Matsubara, H. *J. Biol. Chem.* **1981**, *90*, 1763.

(17) Adman, E.; Watenpugh, K. D.; Jensen, L. H. *Proc. Natl. Acad. Sci. U.S.A.* **1975**, *72*, 4854.

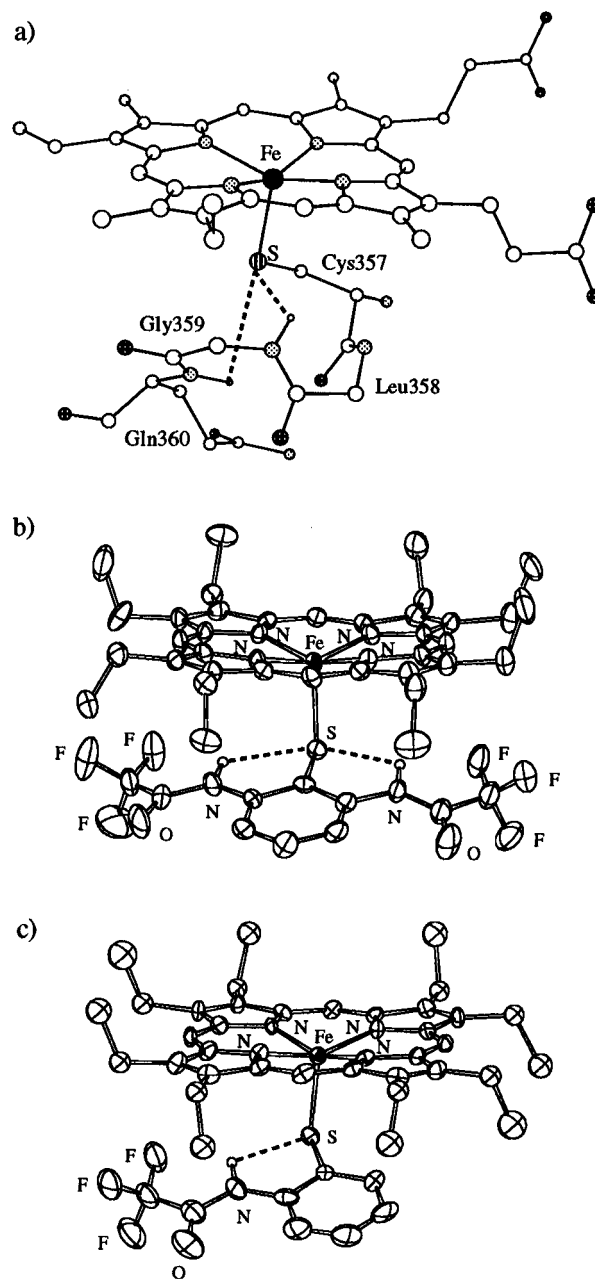


**Figure 1.** Crystal structures of (a) the active site of P-450<sub>cam</sub>,<sup>4</sup> (b) doubly NH···S hydrogen-bonded [Fe<sup>III</sup>(OEP){S-2,6-(CF<sub>3</sub>CONH)<sub>2</sub>C<sub>6</sub>H<sub>3</sub>}] (1), and (c) singly NH···S hydrogen-bonded [Fe<sup>III</sup>(OEP)(S-2-CF<sub>3</sub>CONHC<sub>6</sub>H<sub>4</sub>)] (3).

to investigate the chemical function of NH···S hydrogen bonds in cytochrome P-450, we synthesized novel P-450 iron(III) porphyrin model complexes having intramolecular NH···S hydrogen bonds. This paper communicates the synthesis and properties of novel P-450 model complexes electrochemically modified and remarkably stabilized by single or double NH···S hydrogen bonds.

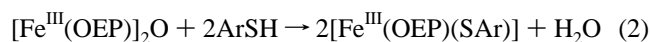
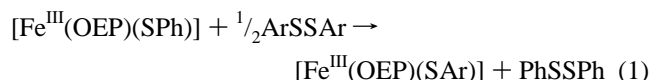
Doubly *ortho*-acylamino-substituted arenethiolates were employed as a Cys thiolate model ligand having two amide dipoles similar to a helix dipole. Thus, [Fe<sup>III</sup>(OEP){S-2,6-(RCONH)<sub>2</sub>-C<sub>6</sub>H<sub>3</sub>}] (R = CF<sub>3</sub> (1), CH<sub>3</sub> (2); OEP = octaethylporphyrinato) was synthesized with a ligand exchange reaction (eq 1) between [Fe<sup>III</sup>(OEP)(SPh)] and the corresponding disulfide {S-2,6-

**Table 1.** Crystal Parameters,  $\nu(\text{NH})$  Shifts, and Redox Potentials of Doubly  $\text{NH}\cdots\text{S}$  Hydrogen-Bonded  $[\text{Fe}^{\text{III}}(\text{OEP})\{\text{S}-2,6-(\text{CF}_3\text{CONH})_2\text{C}_6\text{H}_3\}]$  (**1**), Singly  $\text{NH}\cdots\text{S}$  Hydrogen-Bonded  $[\text{Fe}^{\text{III}}(\text{OEP})(\text{S}-2-\text{CF}_3\text{CONHC}_6\text{H}_4)]$  (**3**) and  $[\text{Fe}^{\text{III}}(\text{OEP})(\text{SPh})]$

	<b>1</b>	<b>3</b>	$[\text{Fe}^{\text{III}}(\text{OEP})(\text{SPh})]^a$
Fe–S <sup>b</sup>	2.356(3)	2.327(4)	2.299(3)
Fe–N <sub>4</sub> plane <sup>b</sup>	0.4142	0.3862	0.466(1)
Fe–S–C <sup>c</sup>	104.5(3)	104.0(5)	102.5(3)
N $\cdots$ S <sup>b</sup>	2.962(9), 2.956(9)	2.93(1)	
$\nu(\text{NH})$ shift <sup>d</sup>	–92 <sup>e</sup>	–123 <sup>f</sup>	
Fe <sup>III</sup> /Fe <sup>II</sup> redox couple <sup>g</sup>	–0.35	–0.52	–0.68

<sup>a</sup> The crystal parameters were quoted from the literature.<sup>22</sup> <sup>b</sup> In angstroms. <sup>c</sup> In degrees. <sup>d</sup> In  $\text{cm}^{-1}$  (KBr disk). <sup>e</sup> Shift from free  $\nu(\text{NH})$  at  $3370\text{ cm}^{-1}$  of  $\{\text{S}-2,6-(\text{CF}_3\text{CONH})_2\text{C}_6\text{H}_3\}_2$  in dichloromethane. <sup>f</sup> Shift from free  $\nu(\text{NH})$  at  $3358\text{ cm}^{-1}$  of  $(\text{S}-2-\text{CF}_3\text{CONHC}_6\text{H}_4)_2$  in dichloromethane. <sup>g</sup> In volts vs SCE in dichloromethane.

$(\text{RCONH})_2\text{C}_6\text{H}_3\}_2^{18}$  (1:0.5), whereas  $[\text{Fe}^{\text{III}}(\text{OEP})(\text{S}-2-\text{RCONHC}_6\text{H}_4)]$  (R =  $\text{CF}_3$  (**3**),  $\text{CH}_3$  (**4**),  $t\text{-Bu}$  (**5**)) was prepared by a reaction (eq 2) between  $[\text{Fe}^{\text{III}}(\text{OEP})]_2\text{O}$  and the thiol, as for  $[\text{Fe}^{\text{III}}(\text{OEP})(\text{S}-4-\text{NO}_2\text{C}_6\text{H}_4)]$ .<sup>19</sup>



(SAr = S-2,6-(RCONH)<sub>2</sub>C<sub>6</sub>H<sub>3</sub> or S-2-RCONHC<sub>6</sub>H<sub>4</sub>)

The molecular structures of **1** and **3** were determined by X-ray analysis to indicate that **1** and **3** possess intramolecular double and single  $\text{NH}\cdots\text{S}$  hydrogen bonds, respectively, as illustrated in Figure 1b,c.<sup>20,21</sup> The selected crystal parameters are listed in Table 1 and compared with those reported for  $[\text{Fe}^{\text{III}}(\text{OEP})(\text{SPh})]$ , implying that the Fe–S bond distance for **1** is longer than those of **3** or  $[\text{Fe}^{\text{III}}(\text{OEP})(\text{SPh})]$ .<sup>22</sup> For Fe(II) and Mo(IV) complexes, the  $\text{NH}\cdots\text{S}$  hydrogen bonding shortens the M–S bond, mainly due to the charge transfer from the antibonding M–S HOMO to amide LUMO.<sup>12,13,23</sup> On the contrary, the hydrogen bonding in **1** and **3** results in a bond elongation, as shown in Table 1. The  $\nu(\text{NH})$  shift in the IR spectra of these complexes also supports the presence of the hydrogen bonds

(18) Ueyama, N.; Yamada, Y.; Okamura, T.; Kimura, S.; Nakamura, A. *Inorg. Chem.* in press.

(19) Tang, S. C.; Koch, S.; Papaefthymiou, G. C.; Foner, S.; Frankel, R. B.; Ibers, J. A.; Holm, R. H. *J. Am. Chem. Soc.* **1976**, *98*, 2414–2434.

(20) Crystal data for  $[\text{Fe}(\text{OEP})\{\text{S}-2,6-(\text{CF}_3\text{CONH})_2\text{C}_6\text{H}_3\}] \cdot \frac{1}{2}\text{C}_7\text{H}_8$ : triclinic,  $PO(1)$ , black plate,  $a = 13.304(4)\text{ \AA}$ ,  $b = 20.151(5)\text{ \AA}$ ,  $c = 9.201(2)\text{ \AA}$ ,  $\alpha = 90.82(2)^\circ$ ,  $\beta = 101.77(2)^\circ$ ,  $\gamma = 100.65(2)^\circ$ ,  $V = 2369(1)\text{ \AA}^3$ ,  $Z = 2$ ,  $D_{\text{calcd}} = 1.354\text{ g cm}^{-3}$ . The structure was refined to  $R = 0.063$ ,  $R_w = 0.069$  for 2965 reflections with  $\text{GOF} = 1.81$ .

(21) Crystal data for  $[\text{Fe}(\text{OEP})(\text{S}-2-\text{CF}_3\text{CONHC}_6\text{H}_4)] \cdot \frac{1}{2}\text{C}_7\text{H}_8$ : triclinic,  $PO(1)$ , black needle,  $a = 13.467(4)\text{ \AA}$ ,  $b = 14.797(6)\text{ \AA}$ ,  $c = 12.821(5)\text{ \AA}$ ,  $\alpha = 103.88(3)^\circ$ ,  $\beta = 107.71(3)^\circ$ ,  $\gamma = 65.94(2)^\circ$ ,  $V = 2202(1)\text{ \AA}^3$ ,  $Z = 2$ ,  $D_{\text{calcd}} = 1.289\text{ g cm}^{-3}$ . The structure was refined to  $R = 0.069$ ,  $R_w = 0.068$  for 2329 reflections with  $\text{GOF} = 1.83$ .

(22) Miller, K. M.; Strouse, C. E. *Acta Crystallogr.* **1984**, *C40*, 1324–1327.

(23) Chung, W. P.; Dewan, J. C.; Walters, M. A. *J. Am. Chem. Soc.* **1991**, *113*, 525–530.

(e.g.,  $-92\text{ cm}^{-1}$  for **1** and  $-123\text{ cm}^{-1}$  for **3**). In the  $^1\text{H}$  NMR spectra of **1–5** in benzene- $d_6$ , the paramagnetically shifted aromatic proton signals appear in the range from  $-100$  to  $70$  ppm, which are characteristic for various high-spin iron(III) porphyrin complexes.<sup>24</sup> The contact-shifted amide NH signals of **1** and **3** are observed at  $-24.8$  and  $-38.1$  ppm due to the direct  $\text{NH}\cdots\text{S}$  hydrogen bond formation.  $[\text{Fe}^{\text{III}}(\text{OEP})(\text{S}-2-\text{CH}_3\text{C}_6\text{H}_4)]$  exhibits methyl protons at  $87.1$  ppm with the opposite contact-shifted spin sign resulting from the  $\pi$ -conjugation. Similarly, the amide NH signal of  $[\text{Fe}^{\text{III}}(\text{OEP})(\text{S}-4-\text{CF}_3\text{CONHC}_6\text{H}_4)]$  was observed at  $30.4$  ppm in  $\text{C}_6\text{D}_6$ .

The Fe–N<sub>4</sub> plane distances of **1** and **3** are shorter compared with that of  $[\text{Fe}^{\text{III}}(\text{OEP})(\text{SPh})]$  reported in Table 1. If the elongation was caused by steric hindrance, the distance between Fe atom and N<sub>4</sub> plane must be elongated as well as the Fe–S bond distance, as found in  $[\text{Co}(\text{TPP})(1\text{-MeIm})]$  and  $[\text{Co}(\text{TPP})(1,2\text{-MeIm})]$ .<sup>25</sup> Actually,  $[\text{Fe}^{\text{III}}(\text{OEP})(\text{S}-2-\text{CH}_3\text{C}_6\text{H}_4)]$  gradually decomposes and is less stable against dioxygen than **1** and **3**. Two bulky thiolate Fe(III) complexes,  $[\text{Fe}^{\text{III}}(\text{OEP})(\text{S}-2,4,6\text{-Me}_3\text{C}_6\text{H}_2)]$  and  $[\text{Fe}^{\text{III}}(\text{OEP})\{\text{S}-2,4,6\text{-}(i\text{-Pr})_3\text{C}_6\text{H}_2\}]$ , are readily reduced to Fe(II) species by their dissociative thiolates to form Fe(II) species. Thus, the steric hindrance of bulky thiolates is not crucial for the stabilization of the Fe(III) state.

The cyclic voltammograms of **1–5** in dichloromethane show a positively shifted Fe<sup>III</sup>/Fe<sup>II</sup> redox couple in the comparison with that ( $-0.68\text{ V}$  vs SCE) of  $[\text{Fe}(\text{OEP})(\text{SPh})]$  without  $\text{NH}\cdots\text{S}$  hydrogen bond by  $0.10\text{--}0.33\text{ V}$ . For example, **1** exhibits the redox couple at  $-0.35\text{ V}$  vs SCE in dichloromethane. These results are consistent with the known fact that the substrate-bound P-450<sub>cam</sub> has a more positively shifted redox potential ( $-0.415\text{ V}$ ) when compared with that ( $-0.572\text{ V}$ ) of substrate-free P-450<sub>cam</sub>.<sup>11</sup>

When **1** and **3** were reduced by tetraethylammonium borohydride, the isolated iron(II) species was found to be detected as  $[\text{Fe}^{\text{II}}(\text{OEP})]$  without axial thiolate. The direct oxidation of **1** by  $\text{PhIO}$  results in the formation of  $[\text{Fe}^{\text{III}}(\text{OEP})]_2\text{O}$ , whereas,  $\text{H}_2\text{O}_2$  decomposes the OEP ligand itself.

Although all the known iron(III) porphyrin thiolato complexes have been reported to be unstable to air and moisture,<sup>19,25</sup> these new complexes are stable against O<sub>2</sub> or H<sub>2</sub>O. For example, **1** is extremely stable in benzene and not oxidized at least for 5 days under air. A polyethylene glycol lauryl ether (10%) aqueous micellar solution ( $0.20\text{ mM}$ ) of **1** is also stable even under similar aerobic conditions. These results indicate that the hydrogen bond plays an important role in the regulation of the stability and reactivity of P-450<sub>cam</sub> in biological systems.

**Acknowledgment.** Support of this work by a Grant-in-Aid for Specially Promoted Research (no. 06101004) from the Ministry of Education, Science, and Culture of Japan is gratefully acknowledged.

**Supporting Information Available:** Tables of non-hydrogen atom anisotropic thermal parameters, complete geometric data and atomic coordinates (17 pages). See any current masthead page for ordering and Internet access instructions.

JA9622970

(24) Arasasingham, R. D.; Balch, A. L.; Cornman, C. R.; Ropp, J. S. d.; Eguchi, K.; Mar, G. N. L. *Inorg. Chem.* **1990**, *29*, 1847–1850.

(25) Scheidt, W. R.; Geiger, D. K.; Lee, Y. J.; Reed, C. A.; Lang, G. J. *Am. Chem. Soc.* **1985**, *107*, 5693–5699.

(26) Ogoshi, H.; Sugimoto, H.; Yoshida, Z. *Tetrahedron Lett.* **1975**, *27*, 2289–2292.